1994

Phase-shift mask issues for 193 nm lithography

Bruce Smith

Suleyman Turgut

Phase-shift mask issues for 193 nm lithography

Bruce W. Smith, Suleyman Turgut
Rochester Institute of Technology
Microelectronic Engineering Department
82 Lomb Memorial Drive
Rochester, New York, 14623-5604

ABSTRACT

As feature sizes below 0.25 micron are pursued, it becomes apparent that there will be few lithographic technologies capable of such resolution. Of these, deep-UV lithography at 193 nm is being investigated, which may prevail over X-ray lithography in terms of manufacturability. Furthermore, through the use of image enhancement techniques such as phase-shift masking, 193 nm lithography may dominate for feature resolution below 0.20 micron. This paper presents results from investigations into phase-shift mask issues for 193 nm excimer laser lithography.

A small field refractive projection system for operation at the 193.3 nm wavelength of a spectrally narrowed ArF excimer laser has been constructed for lithographic research. The small field, 20X system operates with a variable objective lens numerical aperture from 0.30 to 0.60, variable partial coherence, and control over illumination fill. Through the use of attenuated and alternating phase-shifting techniques resolution can be pushed to the 0.2 micron range with depth of focus as large as 2 microns. Problems do arise, though, as these techniques are applied to such short wavelengths of an excimer laser. Sensitivities to shifter deviations and resist interaction increase. Shifter etch influences on fused silica surface characteristics need to be addressed. Transmission effects of attenuating materials becomes increasingly important. Resist imaging and simulation results presented will shed some light on the potential of phase-shift masking for 193 nm lithography, along with inherent difficulties.

1. INTRODUCTION

IC lithography for feature resolution below 0.25 μm is feasible with sub 200 nm exposure sources, which may include the 157 nm F_2 excimer, the 213 nm frequency quintupled Nd:YAG, and the 193 nm ArF excimer lasers. Manufacturability of lithographic processes at these wavelengths, though, becomes increasingly complex. Focal depths as determined by Rayleigh focal depth (λ/NA^2) fall below 1 μm for 0.20 μm resolution using 193 nm exposure and single layer resists. Through the use of multilayer schemes, including bottom anti-reflective coatings, improved process latitude may result in focal depths near 1 μm. Additional image modification techniques may be required for further improvement.

Phase-shift masking has been demonstrated for 365 nm and 248 nm lithography, allowing improvements in both resolution and focal depth. Through *frequency doubling* with alternating phase-shift masking, 0.20 micron resolution may be achieved at 193 nm with focal depths greater than 2μm . Figure 1 shows aerial image log-slope comparisons between a binary mask and an alternating phase-shift mask for 0.2 μm dense features, at 0.45 NA with σ values from 0.1 to 0.9.[1] As can be seen, image log-slope falls below 8 μm^{-1} for the binary mask case for ± 0.4 μm of defocus, even at the highest partial coherence values. An image log slope less than 8 μm^{-1} would not likely be resolved in a single layer resist. For the alternating phase-shift mask case, greater than ±0.8 μm defocus results in an image log slope above 8 μm^{-1} at lower partial coherence values. Alternating phase-shift masking is generally limited for IC lithography to grouped features or grating-like structures. The rim phase-shifting mask[2] is a more practical approach to phase-shift masking, since it is not limited to certain feature

types. Problems inherent with these mask types exist from large feature bias requirements, exposure bias requirements, and the need for additional mask structures. An alternative to the alternating and rim shifting approaches is an attenuated phase-shift mask[3], which creates a phase change in the mask attenuator, fabricated to allow transmission < 10%. The attenuated phase-shift mask shows improvement over a binary mask for dense features, isolated features and contacts. Figure 2 shows image log-slope comparisons between a binary mask and a 6% attenuated mask, at 0.45NA for σ values from 0.1 to 0.9 for isolated 0.2 μm isolated lines. The attenuated phase-shift mask shows increased image log-slope along with a gain in focal depth by as much as 0.2 microns.

Problems arise when considering the processes required to fabricate such phase-shift masks and the resulting influences on linewidth and exposure latitude. Subtractive mask processing through selective removal of fused silica to achieve a π phase shift has been shown to result in linewidth variation greater than 0.05 μm for alternating phase-shift masks.[4] Deviations in phase-shifter thickness has also been shown to effect feature size and exposure latitude. [5] The sensitivity to processing effects at 193 nm is expected to be greater than at 248 nm or 365 nm. Any surface effects resulting from subtractive patterning will have greater impact at shorter wavelengths. Additionally, as etch depths decrease for required π phase shifting (corresponding to 3830Å thickness for 365 nm, 2440 Å for 248 nm ,and 1720 Å for 193 nm) any deviation in shifter thickness is magnified.

Presented here are results from investigations into phase-shift mask issues for 193 nm lithography. Sensitivities of phase-shift masks to surface effects created in subtractive processes will be shown through AFM measurement. Sensitivities to phase-shifter thickness at 193 nm will be presented. Additionally, imaging results will be shown, along with analysis of resolution and focal depth improvements.

2. EXPERIMENTAL

2.1 Imaging system for 193nm

A small field refractive projection system for operation at the 193.3 nm wavelength of a spectrally narrowed ArF excimer laser was utilized for the study[6]. The 20X system operates with a variable objective lens numerical aperture from 0.30 to 0.60, variable partial coherence, and control over illumination fill. A 30 W maximum power ArF excimer laser has been spectrally line-narrowed through incorporation of tilted Fabry-Perot etalons into the laser cavity, allowing linewidths on the order of 7 cm^{-1} (26 pm) with one etalon and 0.5 cm^{-1} (2pm) with two etalons. One etalon operation is sufficient for objective lens NAs below 0.35, calculated for a one half Rayleigh focal depth specification:

$$\Delta\lambda(FWHM) = \frac{(n-1)\lambda}{2f(1+m)(\frac{\partial n}{\partial \lambda})NA^2}.$$

For an NA of 0.45, <12 pm $\Delta\lambda$ is required and for an NA of 0.60, <7 pm $\Delta\lambda$ is required, both obtained with two etalons in the laser cavity.

Polymethylmethacrylate (PMMA) goes through efficient scissioning at 193 nm and was used as the positive resist for this work($n_i = 1.6$). Its high transparency ($\alpha = 0.16\ \mu m^{-1}$)[7] allows for a high degree of interference within thin films, producing standing waves sufficient to severely degrade resolution capability. A low reflective layer of a hard-baked novalac-resin photoresist was coated beneath PMMA films, $n_i = 1.36 - 0.59i$. This reduced reflection at the PMMA/substrate boundaries to 2%. Although some novalac resin swelling was observed during PMMA processing, solubility of novalac in chlorobenzene PMMA casting solvent and IPA/MIBK development solvents is very low and effects were minimal. PMMA films were coated at approximately 0.6 μm. The sensitivity of PMMA at 193 nm is near 1 J/cm^2, requiring maximum source output for reasonable exposure times. This limited excimer spectral narrowing to 26 pm, using one etalon, which delivers ~0.01 w/cm^2 to the

wafer. Irradiance delivered with two etalons is near 1mw/cm^2 , requiring PMMA exposure times of several minutes.

2.2 Subtractive phase-shift mask process

Linewidth variation and loss in exposure latitude not predicted through simulation is a concern in phase-shift mask lithography. Plasma Reactive Ion Etching using F-based chemistry is often used to delineate phase-shifting patterns into fused silica mask substrates. Depending on parameters such as glass structure, thermal history, and surface damage, etching may not be entirely homogenous and anomalies in surface roughness may be produced during etch. Additional surface roughening may result from any etch byproduct deposition on the plasma etched surface. Increased surface roughness may lead to scattering and transmission loss in phase-shifted features. Such optical effects would result in changes in feature size and loss in exposure control - effects which would increase as exposing wavelength decreased. To investigate etch effects on transmission and scattering at 193 nm, a mask grating was designed and electron beam (MEBES) fabricated with grouped features from 0.05 to 1.0 μm (1X) for measurement of image modulation transfer for the 193nm projection system (0.35NA, 0.7σ). Using a 0.1 μm thin layer of PMMA as a threshold detector, image modulation was determined from exposure values required to record mask feature modulation[8] and is shown along with values from simulation in Figure 3. Measurements were made with a chrome on fused silica mask with and without plasma etching in CHF_3 to remove ~2000 Å of silica. To reduce non-uniformity between mask exposures, both etched and unetched quartz gratings were contained on a single mask. AFM measurements of a 1.28 μm x 1.28 μm area of the fused silica without etching and after etching were made and are shown in Figure 4. Additionally, AFM measurements were made on an etched fused silica sample after a 10:1 HF wet etch to remove 100 Å and smooth the plasma etched surface. It is seen that the plasma RIE in CHF_3 (100 sccm, 50mTorr, 100W) resulted in a large amount of surface roughening of the fused silica. Roughness of the unetched sample is within the error of the system (noise st. dev. was approximately 20 Å). After etching to remove ~2000 Å, surface roughness increased, with ranges greater than 200 Å. It should be noted that samples were etched using chrome as a mask rather than resist, reducing the likelihood of redeposition of surface contaminants. After 10:1 HF smoothing, roughness was reduced to ranges less than 100 Å. Although the etched quartz pattern produced a loss of transmission of near 5%, no measurable loss in modulation was realized. The transmission loss is great enough to produce linewidth loss and a decrease in exposure latitude in a phase-shift mask process, which was investigated and will be presented.

2.3 Phase errors at 193 nm

Errors in phase-shifter thickness scale with wavelength. At 365 nm, a 10° phase-shifter error translates to 212 Å thickness (n = 1.47). At 193 nm, 10 ° error results from a thickness error of 96 Å (n = 1.56) , less than half of the thickness for 365 nm. Simulations for ± 5°, ±10°, and ±20° are shown in Figure 5, corresponding to ±48 Å, ±96 Å, and ±192 Å. Shown are results for 0.2 micron dense lines using an alternating phase-shift mask, 0.45NA, 0.3σ. A ±10° phase-shift error (±96 Å) causes a 0.4 μm loss of focal depth for an aerial image log slope of 8 μm^{-1}. Resist sensitivity to shifter errors has been shown to be mode-dependant, with negative resists being more sensitive to shifter deviations than positive resists.[5] Control of shifter etch depth as determined by exposure and focus latitude requirements may prove difficult in subtractive phase-shift mask processes.

2.4 Alternating 193 nm phase-shift mask

An alternating phase-shift mask was fabricated at 20X using combined electron beam and optical techniques, incorporating dense features down to 0.20 μm. Because of the large reduction value of the mask and the small shifter depth required for π phase-shift at 193 nm (1720 Å), an HF shifter etch was utilized to minimize transmission losses introduced with plasma RIE etching. Chromium has a reflectivity of 44.7% at 193 nm, as compared to the 65.7% at 365 nm, and no mask AR layer was used[9]. Fused silica was subtractively etched to 1700 Å ± 100 Å as measured with a surface profilometer. Imaging of the mask was done at 193 nm using a 0.35 NA on the variable NA projection system. The alternating phase-shifting effectively doubles the cut-off frequency for an imaging system, allowing use of lower coherence values for features below k_1= 0.5. A σ of 0.3 was chosen to maximize image modulation while maintaining reasonable irradiance at the wafer.

Development rate and exposure parameters for PMMA were incorporated into a lithographic modeling package[1] to allow simulation of resist imaging effects. Figure 6 shows results of imaging 0.24 μm features in PMMA along with simulation results for a ±10% variation around an optimal exposure dose. Results show a 2 μm focal depth for features while maintaining a 14% CD tolerance. Figure 7 shows a SEM image of 0.24 μm dense lines at 1 μm defocus. A linewidth difference of 0.01 μm is detected between phase-shifted and non phase-shifted regions, an occurrence which was not anticipated with the HF etch process used. It is expected that a shifter edge effect produced at or beneath the chrome features along with a transmission loss in etched regions have contributed to the deviation.

2.5 Attenuated 193 nm phase-shift mask

Utilizing a mask attenuator that has some degree of transmission, a phase-shift can be obtained between "opaque" and "transparent" areas. Attenuated phase-shift masking has potential for use with isolated lines, contacts, and dense features, with less layout and process complexity. Figure 8 shows the increase in image log-slope obtained for 0.2 micron isolated lines using 193 nm at 0.45NA and σ = 0.7. Using a minimum image log-slope of 8μm^{-1} for a single layer resist, an improvement of 0.15 μm in focal depth can be realized for a 6% transmitting phase-shift mask verses a binary mask (0% transmitting).

Partially transmitting chrome on fused silica was prepared for mask fabrication by sputtering Cr films of ~800 Å and wet etching until desired transmission values at 193 nm were achieved. Chrome films of 2%, 6%, and 9% were produced, and coated with 0.5 μm of a novalac-based electron beam resist. Isolated and dense features down to 0.10 μm were e-beam patterned, developed, chrome etched and followed by an HF phase-shift etch of 180° ± 100Å.

Imaging was performed at 193 nm using a 0.35 NA on the variable NA projection system. A σ of 0.7 was chosen to maximize image modulation, with 0.30 μm features corresponding to k_1 of 0.54 for the imaging set-up. Results from the 6% attenuated mask are shown in Figure 9 and SEM results for ±0.5 μm defocus are shown in Figure 10. Dense lines of 0.30 μm in PMMA are shown with simulation results for ±10% variation around optimal exposure dose. Nearly 2μm in focal depth is predicted from simulation for a 10% linewidth tolerance. Experimental results show depths less than 1.5 μm, which might be improved through better exposure and focus control. Linewidth bias is greater for experimental results than predicted, which may substantiate this.

3. CONCLUSIONS

Results obtained from alternating and attenuated phase-shift masks show potential for application to 193nm lithography. Resolution to 0.3 μm using a 6% attenuated phase-shift mask and to 0.24 μm using an alternating phase-shift mask have been demonstrated with 0.35 NA, resulting in focal depths on the order of 1.5 to 2μm. An increase in objective lens NA to 0.45 has potential for resolution to 0.20 micron, while maintaining focal depths well above 1.5 μm. Although the attenuating phase-shift mask introduces little additional mask design and process complexity, defect issues may make them less attractive for manufacturing. Increased pinhole density along with difficult inspection and repair requirements will be an important issue. Alternative attenuating materials may require investigation. Imaging at 193 nm is also more sensitive to subtractive etch processes and may require use of alternative shifter materials and patterning schemes. Additionally, resist loss in dark regions may require that the optical properties of resist be carefully optimized, which is difficult with the current few choices in resist materials for 193nm exposure.

4. ACKNOWLEDGMENTS

The authors would like to thank Scott Blondell, Ricardo Toledo-Crow, and Joe Summa for their assistance with this work.

5. REFERENCES

[1] Simulations performed with PROLITH/2 V2.2. FINLE Technologies.

[2] A. Nitayama, T. Sato, K, Hasimoto, F. Shigenmitsu, M. Nakase, IEDM Tech. Dig., (1989), p. 57.

[3] H.I. Smith, E.H. Anderson, M.L. Schattenburg, U.S. Patent 4,890,309.

[4] R.L. Kostelak, C. Pierrat, J.G. Garofalo, S. Vaidya, J. Vac. Sci. Technol. B. 10(6), (1992), p. 3055.

[5] K. Ronse, R. Jonckheere, K. Baik, R. Pforr, L. Van den hove, J. Vac. Sci Technol. B, 10(6), (1992), p. 3012.

[6] B.W. Smith, M.C. Gower, M. Westcott, L. Fuller, SPIE Vol. 1927, Optical / Laser Microlithography VI, (1993), p. 914.

[7] Optical properties of materials at 193nm provided by R. Kunz.

[8] A. Grassman, H. Moritz, J. Vac. Sci. Technol. B 10(6), (1992), p. 3008.

[9] Reflectivity data for chromium from CRC Handbook of Chemistry and Physics, 72nd edition.

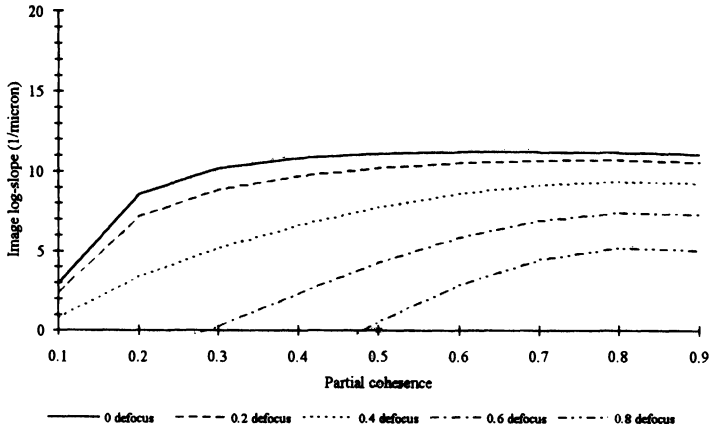

Figure 1a. Image log-slope vs. partial coherence for binary mask, 0.2 μm dense lines, 193 nm, 0.45 NA.

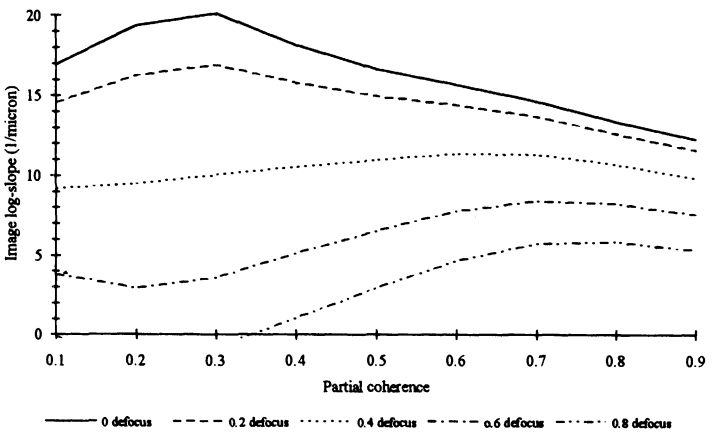

Figure 2a. Image log-slope vs. partial coherence for binary mask, 0.2 micron isolated lines, 193 nm, 0.45NA.

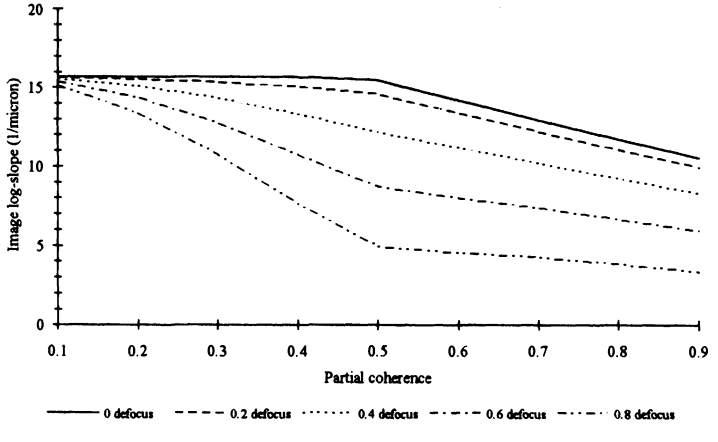

Figure 1b. Image log-slope vs. partial coherence for alternating phase-shift 0.2 micron dense lines, 193 nm, 0.45NA.

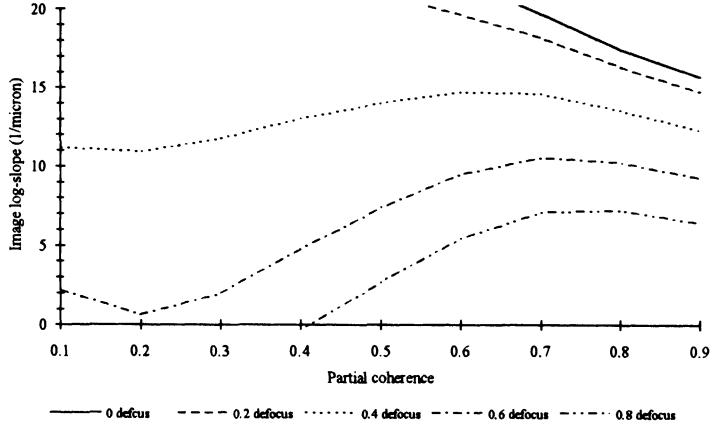

Figure 2b. Image log-slope vs. partial coherence for 6% attenuated phase-shift 0.2 μm isolated lines, 193 nm, 0.45 NA.

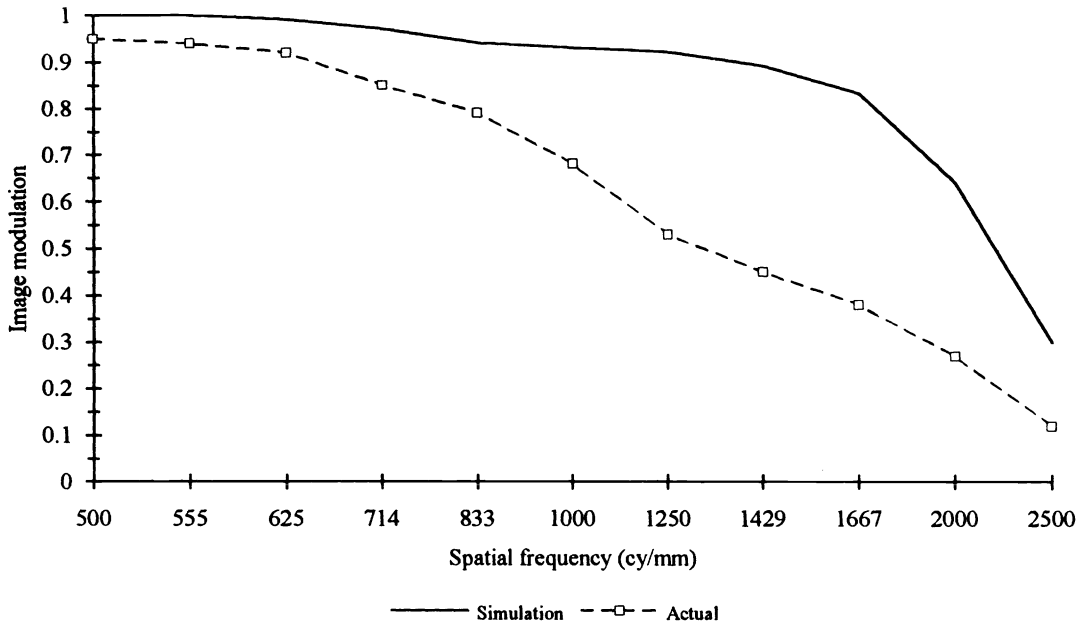

Figure 3. Image modulation for 193 nm, 0.35 NA projection system, $\sigma = 0.7$.

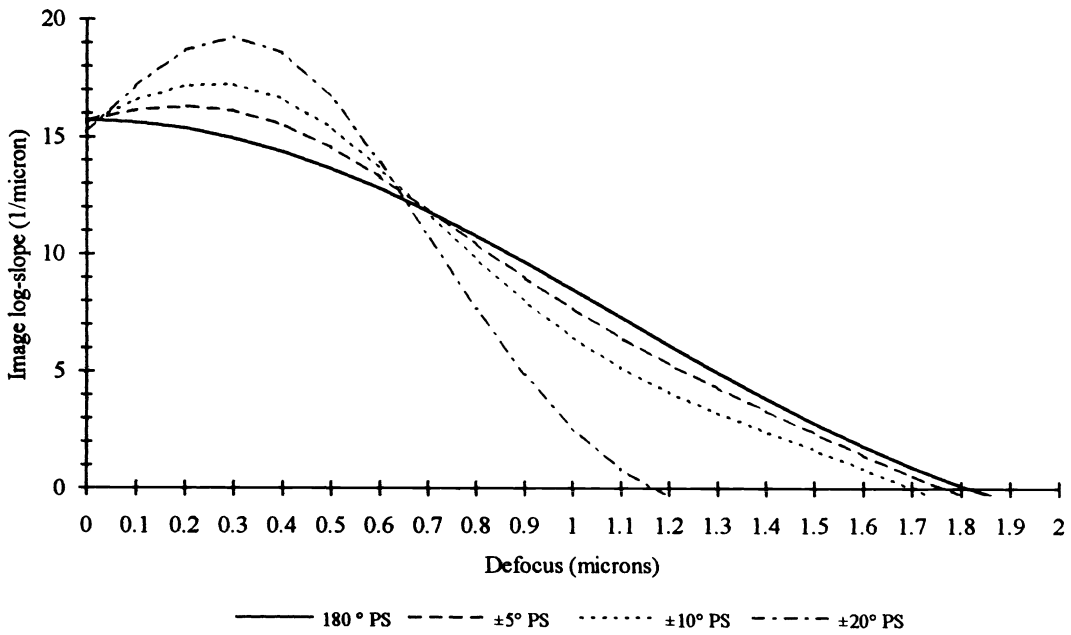

Figure 5. Image log-slope vs. defocus for alternating phase-shift mask, 0.2 μm dense lines, 193 nm, 0.45NA, σ=0.3, with ±5°, ±10°, and ±20° phase-shift errors.

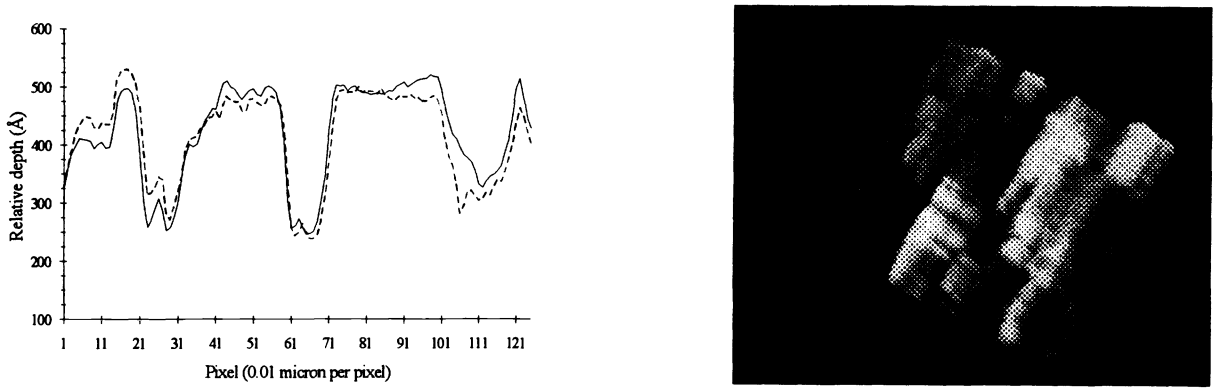

Figure 4a. AFM measurement (1.28x1.28 μm) of fused silica, RIE CHF_3 etched 2000 Å.

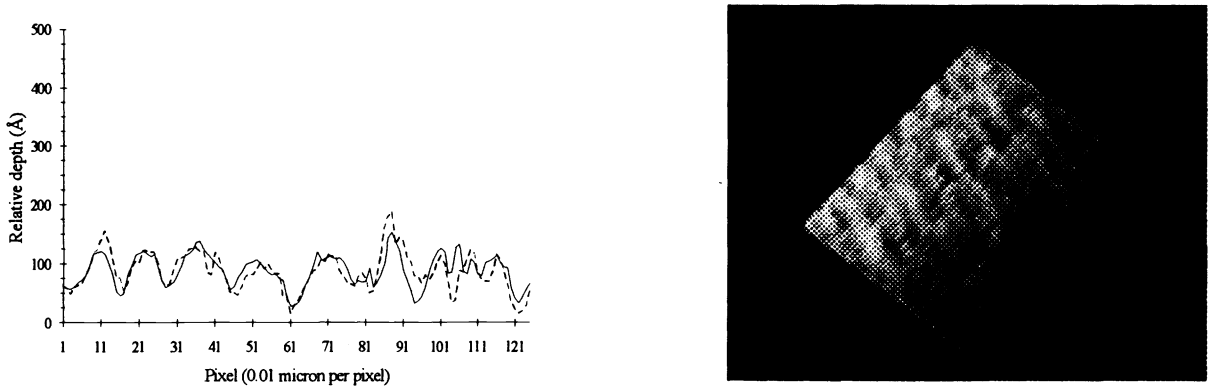

Figure 4b. AFM measurement of fused silica, RIE CHF_3 etched 2000 Å, 10:1 HF smoothed 100 Å.

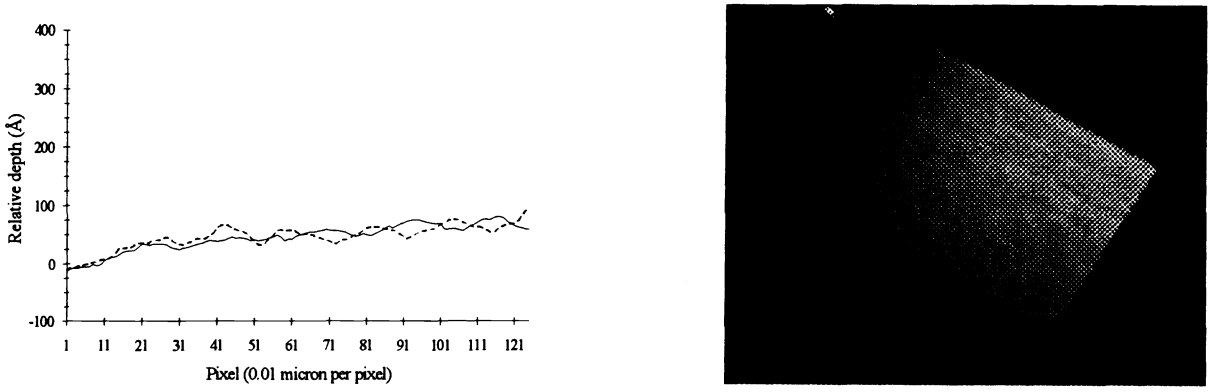

Figure 4c. AFM measurement of fused silica, no etch.

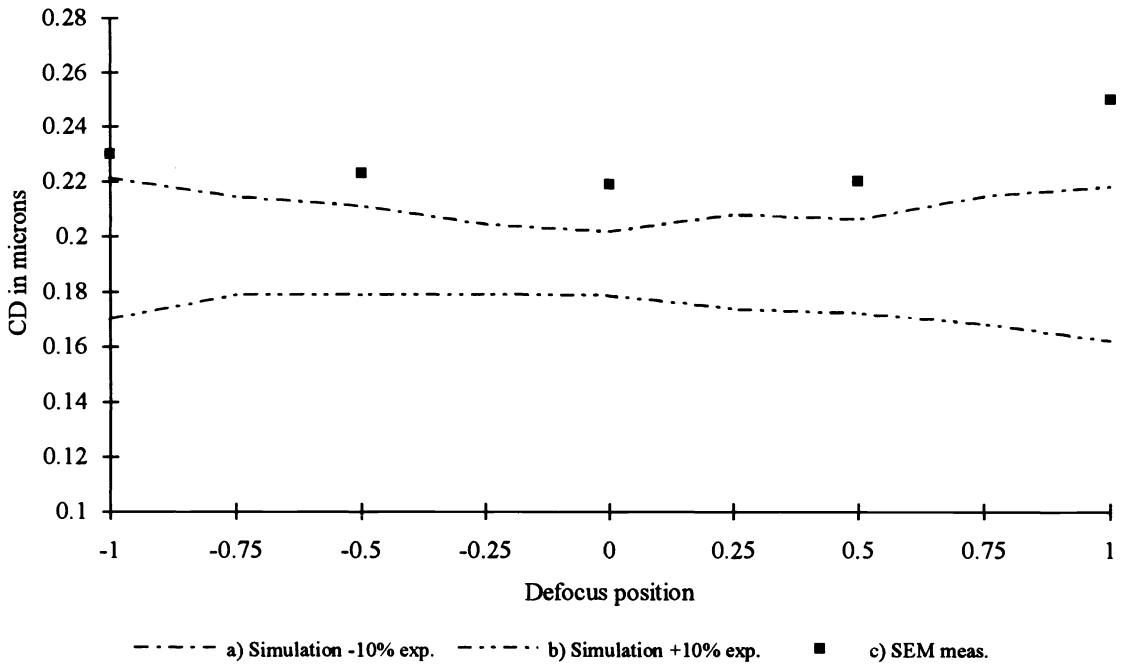

Figure 6. 0.24 micron dense lines imaged with alternating phase-shift mask.

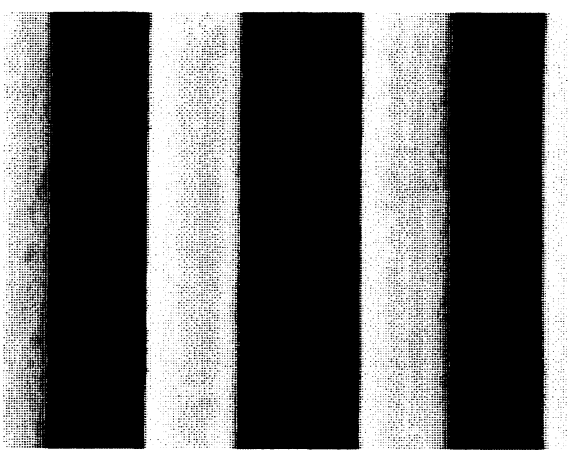

Figure 7. SEM of 0.24 dense lines at 1 μm defocus, showing linewidth variation from shifter etch.

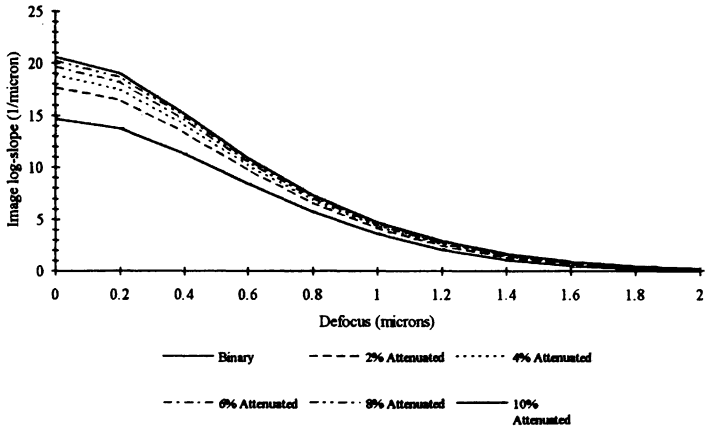

Figure 8. Image log-slope for attenuated phase-shift mask, 0.2 μm isolated lines, 193 nm, 0.45NA, σ=0.7.

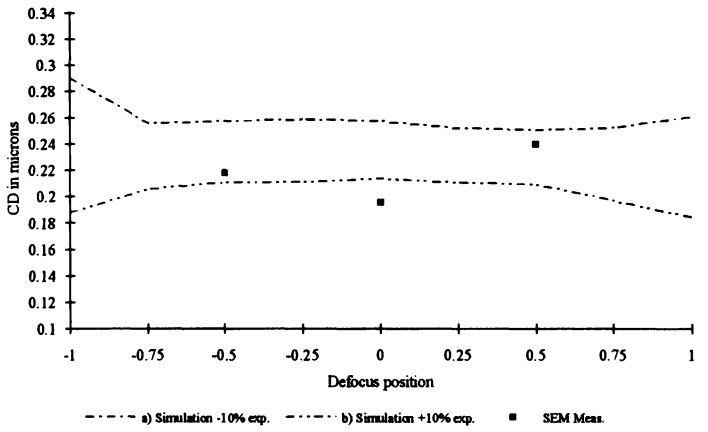

Figure 9. 0.30 micron dense lines imaged with 6% attenuated phase-shift mask.

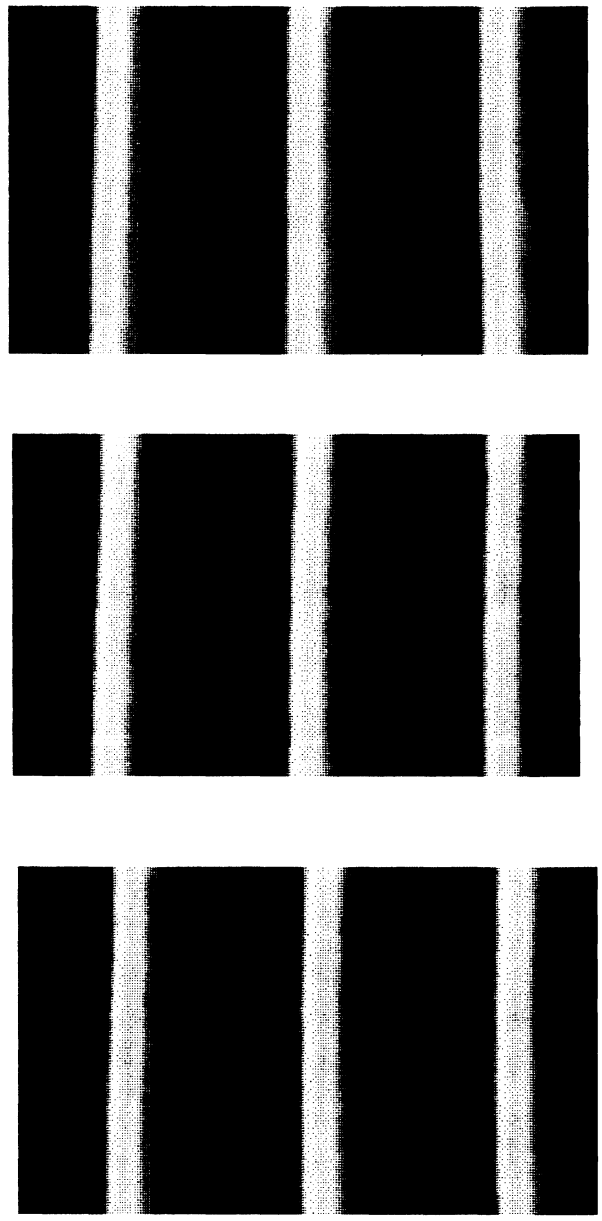

Figure 10. SEM of 0.30 μm dense lines imaged with 6% attenuating pahse-shift mask.

+0.5 μm defocus

Best focus

-0.5 μm defocus